Geophysical Research Letters

RESEARCH LETTER
10.1029/2025GL116107

Infrasound Unmasks Flow Turbulence as an Additional Seismic Source in Debris Flows

Giacomo Belli[1], **Emanuele Marchetti**[1], **Fabian Walter**[2], **and Duccio Gheri**[1]

[1]Department of Earth Science, University of Florence, Florence, Italy, [2]Swiss Federal Institute for Forest, Snow and Landscape Research (WSL), Zurich, Switzerland

Key Points:

- Infrasound by debris flows is radiated by turbulence-induced waves at flow surface mostly generated at significant channel irregularities
- Seismo-acoustic cross-correlation suggests that, in addition to particle collisions, turbulent flow radiates seismic waves in debris flows
- Infrasonic array processing and seismo-acoustic cross-correlation analysis can be used to track and detect debris flows

Supporting Information:

Supporting Information may be found in the online version of this article.

Correspondence to:

G. Belli,
g.belli@unifi.it

Citation:

Belli, G., Marchetti, E., Walter, F., & Gheri, D. (2025). Infrasound unmasks flow turbulence as an additional seismic source in debris flows. *Geophysical Research Letters*, *52*, e2025GL116107. https://doi.org/10.1029/2025GL116107

Received 21 MAR 2025
Accepted 14 APR 2025

Author Contributions:

Conceptualization: Giacomo Belli, Emanuele Marchetti, Fabian Walter
Data curation: Giacomo Belli, Emanuele Marchetti, Fabian Walter, Duccio Gheri
Formal analysis: Giacomo Belli
Funding acquisition: Emanuele Marchetti
Investigation: Giacomo Belli, Emanuele Marchetti, Fabian Walter, Duccio Gheri
Methodology: Giacomo Belli, Emanuele Marchetti
Project administration: Emanuele Marchetti
Resources: Emanuele Marchetti, Fabian Walter
Software: Giacomo Belli
Supervision: Emanuele Marchetti

Abstract Debris flows radiate both seismic and infrasonic waves. According to previous studies, seismic energy is generated by the solid particle collisions with the riverbed and is dominated by the boulder-rich front, while infrasound is produced by turbulence-induced waves at the flow surface. To further investigate this complex radiation processes, we present the seismo-acoustic analysis of a debris-flow event at Illgraben (Switzerland). Array processing shows that infrasound is preferentially radiated at channel irregularities, acting as predominant acoustic sources because of the intense flow turbulence. The high crosscorrelation observed between the recorded infrasonic and seismic signals suggests that, in addition to the dominant source related to particle impacts, a minor seismic component is produced by the flow waves developing at topographic steps.

Plain Language Summary Debris flows represent a major hazard in mountain environments. While flowing, debris flows generate both seismic waves and infrasound (low-frequency sound). According to previous studies, the seismic waves are produced by the collision between the transported debris and the riverbed, while infrasound is generated by the flow waves developing at its surface. Here we present a combined analysis of the infrasonic and seismic signals generated by a debris-flow event at Illgraben (Switzerland). The analysis reveals that the infrasound is preferentially produced when the flow overruns the check dams and flow waves develop downstream. These latter also produce seismic waves, which, despite being weaker, add to the dominant seismic component produced by particle collisions. Eventually we show how seismo-acoustic signals can be used to track the debris flow along the channel.

1. Introduction

Debris flows are episodic, fast torrent-floods carrying large amounts of solid debris and boulders (Coussot & Meunier, 1996; Iverson, 1997), typically occurring within steep mountain catchments as a result of a sudden water supply (Berti & Simoni, 2005). They represent one of the major natural hazards in worldwide mountain environments (Dowling & Santi, 2014).

Over the last 20 years, the use of seismo-acoustic sensors has gained attention for monitoring debris flows and investigating their dynamics (Arattano & Marchi, 2008; Belli et al., 2022; Burtin et al., 2009, 2014; Coviello et al., 2019; Marchetti et al., 2019; Lai et al., 2018; Walter et al., 2017). Similar to other mass movements, such as snow avalanches (Belli et al., 2025; Havens et al., 2014; Johnson et al., 2021; Kogelnig et al., 2011) and pyroclastic density currents (Allstadt et al., 2019; Delle Donne et al., 2014), debris flows radiate elastic energy both in the ground, in the form of seismic waves (Burtin et al., 2009; Lai et al., 2018; Walter et al., 2017), and in the atmosphere, as infrasound (low frequency sound, <20 Hz) (Belli et al., 2022; Kogelnig et al., 2014; Marchetti et al., 2019; Schimmel & Hübl, 2016).

The seismic observation of debris flows has been addressed in several studies, focusing both on event characterization and detection (Allstadt et al., 2019; Arattano & Marchi, 2008; Belli et al., 2022; Bessason et al., 2007; Coviello et al., 2019; Walter et al., 2017) and on the investigation of the seismic source mechanisms (Burtin et al., 2009, 2014; Kean et al., 2015; Lai et al., 2018; Zhang, Walter, McArdell, Wenner, et al., 2021). Both theoretical and experimental studies suggest that the seismic radiation by debris flows is similar to what is observed for rivers (Burtin et al., 2008; Gimbert et al., 2014; Schmandt et al., 2013; Tsai et al., 2012), where seismic waves are radiated by bedload transport and turbulent-flow structures. The most accepted source models on debris-flow seismicity are based on the work by Tsai et al. (2012) on the generation of seismic energy by bedload transport in rivers, and attribute the radiation of seismic waves to solid particle collisions with the riverbed (Farin et al., 2019; Kean et al., 2015; Lai et al., 2018; Zhang, Walter, McArdell, Wenner, et al., 2021):

Validation: Giacomo Belli, Emanuele Marchetti, Fabian Walter
Visualization: Giacomo Belli
Writing – original draft: Giacomo Belli
Writing – review & editing: Giacomo Belli, Emanuele Marchetti, Fabian Walter, Duccio Gheri

Collisions induce stress oscillations in the ground, generating seismic surface waves. For debris flows, the boulder-rich flow front, where most of the largest boulders concentrate, dominates the produced seismic signal (Farin et al., 2019; Walter et al., 2017).

The use of infrasonic signals to study and monitor debris flows is quite recent (∼15 years). To date, most efforts have been limited to event detection, using infrasound for early warning purposes (Schimmel & Hübl, 2015; Liu et al., 2015, 2018), sometimes combined with seismic signals (Schimmel & Hübl, 2016). Only a few attempts have been aimed at investigating the infrasonic source mechanism in debris flows (Belli et al., 2022; Coco et al., 2021; Marchetti et al., 2019). These studies all agree that infrasound is generated by turbulence-induced waves and splashes developing at the debris-flow free surface, which collide with the air, producing small stress oscillations propagating in the atmosphere as low-frequency pressure waves (Belli et al., 2022; Coco et al., 2021; Marchetti et al., 2019). According to fluid-dynamics, these surface oscillations are preferentially produced at channel irregularities (Belli et al., 2022; Chaudhry, 2008; Feng et al., 2014; Henderson, 1996; Tokyay & Yildiz, 2007).

Although previous works have highlighted that in debris flows seismic and infrasonic signals are produced by different decoupled processes (Belli et al., 2022; Marchetti et al., 2019), their spatial and temporal relationship has not been investigated in detail yet. A debris flow is indeed an extended seismo-acoustic source, where seismic waves and infrasound are produced at the same time in different locations (Belli et al., 2022; Farin et al., 2019; Marchetti et al., 2019). Moreover, seismo-acoustic coupling makes the analysis even more complicated (Ichihara et al., 2012), as infrasound transmits in the ground as seismic waves (de Groot-Hedlin & Hedlin, 2019; Novoselov et al., 2020) and seismic waves transfer into the air as infrasound (Marchetti et al., 2016; Mutschlecner & Whitaker, 2005). This means that what is recorded by a seismic sensor may not correspond only to the primary signal (i.e., signal produced directly by the source), but may include or consist only of the secondary component produced by the transmission in the ground of primary infrasound nearby the receiver (Hicks et al., 2023; Le Pichon et al., 2021); the same holds for infrasound (Kim et al., 2004). The effectiveness of seismo-acoustic coupling can be evaluated by a cross-correlation analysis between the recorded infrasound and seismic signals (Ichihara et al., 2012). This analysis allows us also to investigate the interconnection between primary infrasonic and seismic signals, sometimes also highlighting additional source mechanisms for the analyzed wavefields (Matoza & Fee, 2014).

This study presents the combined seismo-acoustic analysis of a debris flow occurred at Illgraben (Switzerland, Canton Valais) on 15 July 2019 and recorded by an infrasonic array and a co-located seismometer. Seismic and infrasonic signals are analyzed in the frequency domain, and infrasound is further analyzed with array processing techniques to investigate and locate its source mechanism. We also perform seismo-acoustic crosscorrelation analysis to investigate the relation between the recorded signals. Results allow us to define additional constraints on the seismo-acoustic energy radiation by debris flows and suggest how the signals can be used to track events along the channel.

2. Study Site and Data

The Illgraben (Figure 1b) is one of the most active and best-instrumented debrisflow catchments worldwide, producing every year an average of 4–6 events capable of transporting meter-sized boulders, with flow heights up to a few meters and total volumes commonly exceeding few tens of thousands of cubic meters (Badoux et al., 2009; McArdell et al., 2007). The basin is drained by the Illgraben torrent and has a total area of ∼10 km^2, almost equally divided between the steep upper catchment, which is the source area of the sediment feeding the debris flows, and the densely inhabited debris fan in the Rhone valley (Schlunegger et al., 2009). In the 1960s, 30 check dams (CD, hydraulic engineering work built transversal to the riverbed to reduce flow energy; Figures 1b–1e), including a ∼50 m high dam in the upper basin, were constructed to stabilize the channel and dampen debris flow impact.

In this work, we analyze the Illgraben debris flow on 15 July 2019 (Figures 1c–1e). The event was recorded with a maximum flow depth (measured at CD29) of ∼0.54 m, a front velocity (computed from arrival times at CD27 and 29) of 3.4 m/s, a bulk density (estimated with the force plate installed at CD29, (McArdell et al., 2007)) of ∼2,200 kg/m^3, and a total volume of ∼9,900 m^3 (Belli et al., 2022).

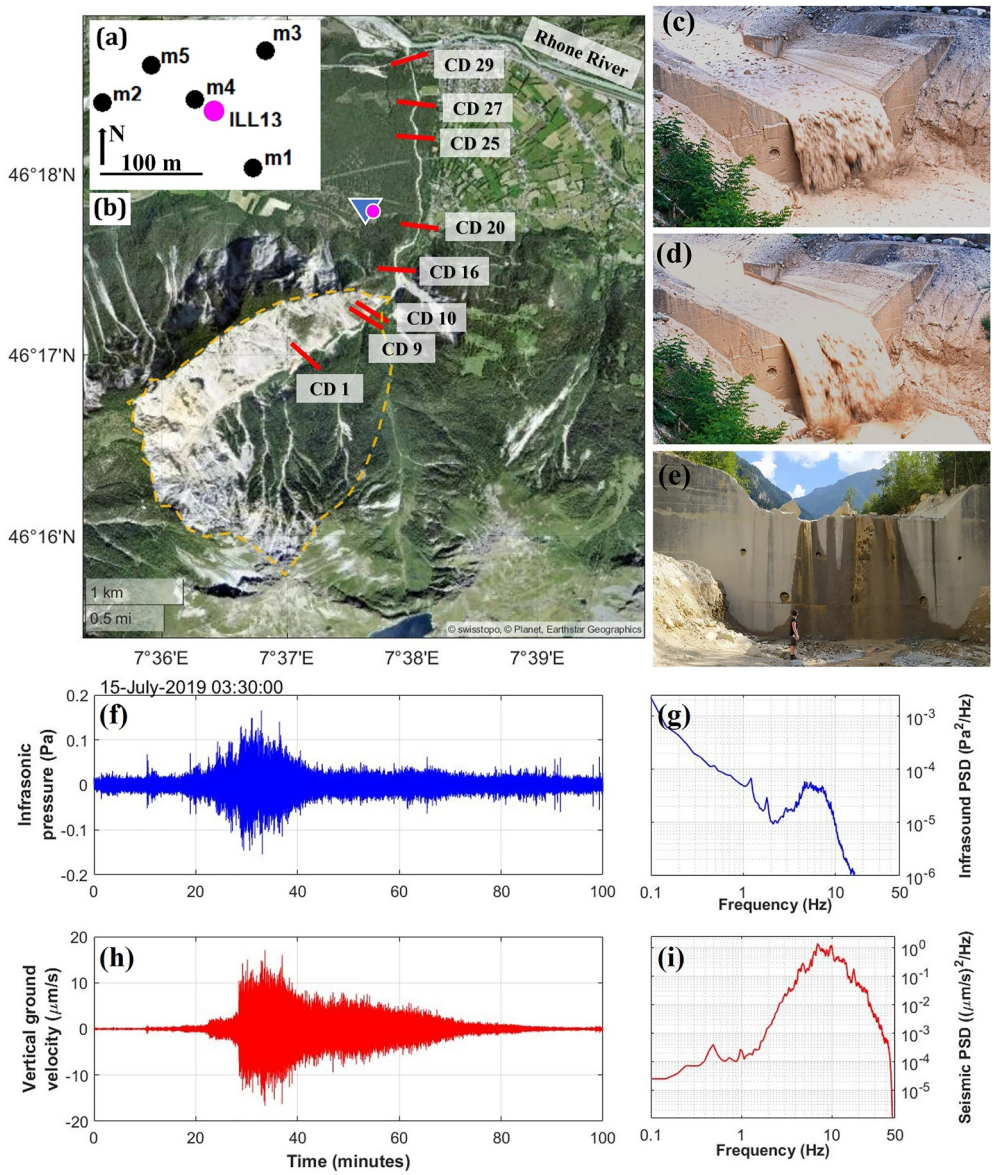

Figure 1. Map of the Illgraben catchment (b). The dashed orange line highlights the upper catchment. Red bars with alphanumeric code indicate the location of some check dams (CD). The blue triangle marks the location of the ILG infrasonic array, whose geometry is shown in panel a, while the magenta circle indicates the position of the ILL13 seismic station. Two frames of the debris-flow event on 15 July 2023 flowing over the ~4 m high CD29 (c, d; source: WSL). Photo of the ~8 m high CD20 (e; source: Unifi). 1–20 Hz filtered infrasonic (f) and 1–40 Hz filtered seismic (h) signals generated by the 15 July 2019 event. Infrasonic (g) and seismic (i) power spectral densities (PSD).

For this study we use infrasound data recorded with an infrasonic array (ILG) deployed in a flat forested area on the Illgraben debris fan at a distance of ~550 m from the channel (46°17'49.02"N, 7°37'38.72"E) (Figure 1b). The array consists of five infrasonic sensors arranged into a roughly triangular geometry (Figure 1a), with an aperture (maximum distance between two elements) of ~160 m, optimized to analyze infrasound signals in the frequency band between 1 and 10 Hz. Each sensor is deployed inside a plastic barrel buried in the ground and equipped with a differential pressure transducer with a sensitivity of 400 mV/Pa in the pressure range of ±12.5 Pa and a flat frequency response between 0.01 and 200 Hz. Pressure data are collected at 50 Hz at each element of the array and then transmitted through fiber optic cables to the FIBRA digitizer (www.itemgeophysics.it).

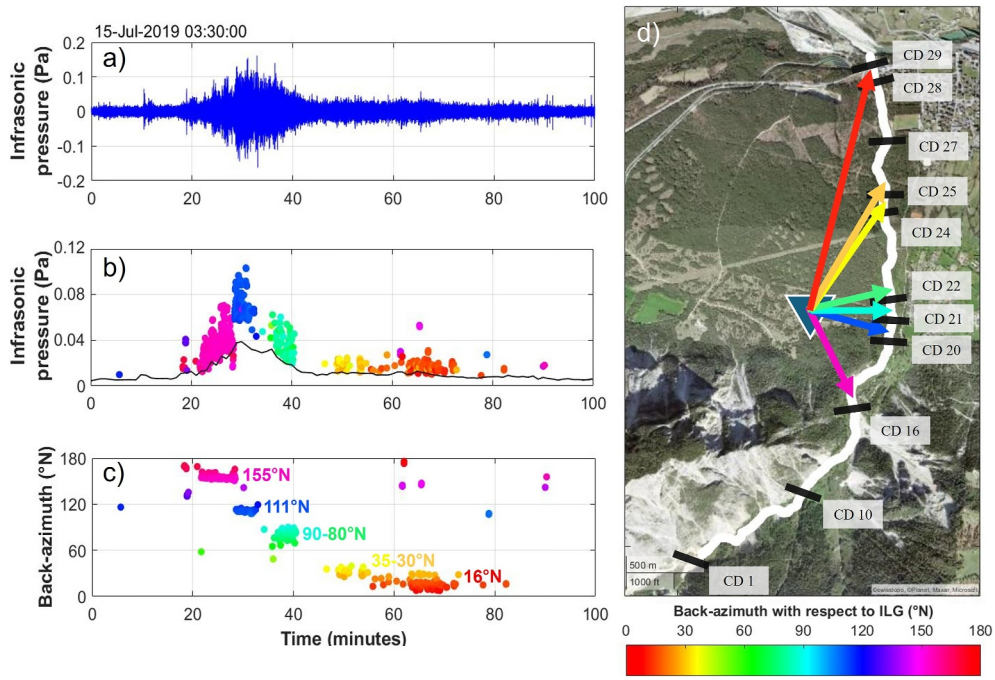

Figure 2. Infrasonic array processing of the Illgraben debris flow on 15 July 2019. 2–10 Hz band-pass filtered infrasonic track recorded at M1 (a); infrasonic pressure (b) and back-azimuth (c) computed with the array processing. The black line in panel b represents the root mean square amplitude envelope of the infrasonic signal computed over 1-min windows (see Section S2 in Supporting Information S1). Map of the Illgraben channel between CD1 and CD30 showing the location of ILG array (blue triangle) and check dams (CD, black bars) (d). Arrows in panels (d) point in the directions indicated by the back-azimuth values highlighted in (c). Colors in panels (b), (c) and (d) all refer to the color bar below diagram (d).

We also use seismic data collected by a temporary station, part of the dense seismic network deployed at Illgraben during the debris-flow season since 2017 (Wenner et al., 2019). The seismic station, named ILL13, is deployed within 10 m from the central element of the infrasonic array (m4, Figures 1a and 1b) and is equipped with a Lennartz LE-3Dlite seismometer with a flat response between 1 and 80 Hz. The sensor is placed into a 30 cm deep pit filled up with sand. Ground velocity is recorded with a Nanometrics Centaur digitizer at 100 Hz.

3. Methods

We perform spectral analysis of recorded seismo-acoustic signals computing power spectral densities (PSD; Figures 1g and 1i) and spectrograms (Figure S1 in Supporting Information S1) on raw infrasonic and seismic data, using moving data windows of 20 s over the entire signal duration.

Then, to investigate the infrasonic source mechanism within debris flows, recorded infrasound is analyzed by applying array processing (Figure 2). The use of an array allows to reconstruct the direction from which the infrasonic ray comes from, expressed by the back-azimuth (i.e., planar direction of the infrasonic wave with respect to the array, computed based on the recording-time differences of the signal at the different sensors), thus providing crucial information on the position of the source. We use the procedure described by Belli et al. (2021), based on the cross-correlation of the data recorded at all the sensors of the array. The processing is performed over 10-s moving signal windows with 90% of overlap, in the 2–10 Hz frequency band, centered on infrasound peak frequency (see Figure 1g). Within each window, if the correlation between the data recorded at all sensors of the array is higher than a fixed threshold, an infrasonic detection is defined and characterized in terms of pressure and back-azimuth. The processing used here is able to identify in each moment only the infrasound component recorded as the most energetic at that time.

To explore the interconnection between the seismo-acoustic signals radiated by debris flows, we perform the cross-correlation analysis between the seismic signal recorded at ILL13 and the infrasonic data acquired at the central element (m4) of ILG array. This allows us to compare signals recorded at the same location, since m4 and

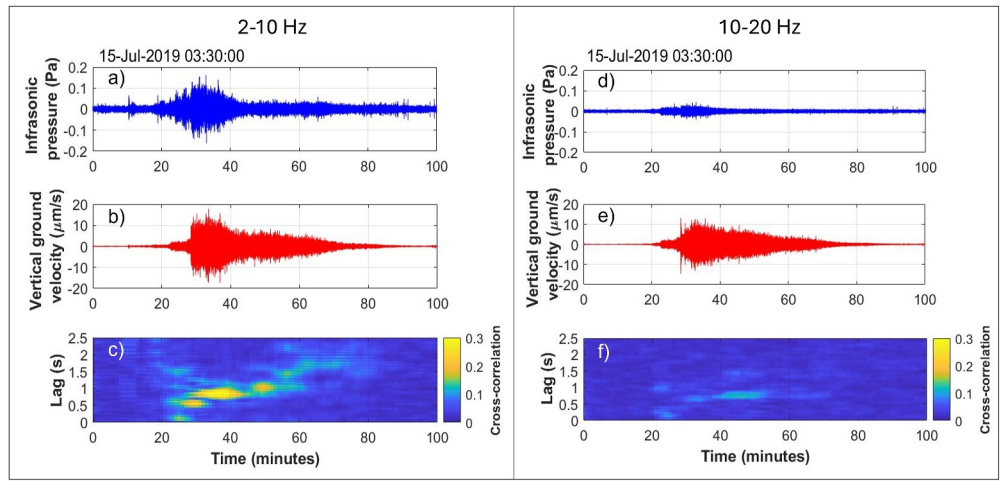

Figure 3. Infrasonic (a, d) and seismic (b, e) signals and corresponding seismo-acoustic crosscorrelation (c, f) computed in the 2–10 Hz (left column) and 10–20 Hz (right) frequency bands.

ILL13 are less than 10 m apart (Figure 1a). The seismo-acoustic cross-correlation is computed on 1 min moving signal windows along the entire signal duration, in two different frequency bands: 2–10 Hz (Figures 3a–3c), where most of the infrasonic energy is concentrated (Figures 1g and 3a), and 10–20 Hz (Figures 3d–3f), for which high seismic energy (Figure 3e) but little infrasound (Figure 3d) are recorded.

4. Results and Discussion

4.1. Spectral Analysis

The 15 July 2019 debris flow generated ∼1-hr-long seismic and infrasonic signals. While infrasound shows a symmetric cigar-shaped signal (Figure 1f), the seismic envelope is rather asymmetric, characterized by a steep onset and a more gradual and longer coda (Figure 1h).

The spectral analysis of the signals reveals significantly different frequency contents; while the infrasonic energy is concentrated in the 2–10 Hz band and peaks around 6 Hz (Figure 1g), the seismic radiation is widely distributed between 1 and 40 Hz and peaks around 7.3 Hz (Figure 1i) (Belli et al., 2022). According to previous models (Lai et al., 2018; Tsai et al., 2012), the seismic spectral content by debris flows strongly depends on wave attenuation and source-to-receiver distance, this latter determining the recorded seismic peak frequency. Nevertheless, Belli et al. (2022) showed that the discrepancy observed between the recorded infrasonic and seismic frequency footprints, observed for several Illgraben events, is not due to site or propagation effects, but would result also for signals recorded at the source (Zhang, Walter, McArdell, de Haas et al., 2021). The different spectral contents therefore corroborate the idea that the two wavefields are dominated by different decoupled source processes, simultaneously acting at the flow-air interface and at the riverbed.

4.2. Infrasonic Array Processing

Array processing shows that the recorded infrasonic signal is dominated by ∼5–10 min clusters of coherent infrasound (Figure 2), each characterized by almost constant back-azimuth values, which vary from cluster to cluster (Figure 2c). This indicates that most of the infrasonic energy by the debris flow is radiated from different fixed positions along the channel.

The computed back-azimuth values (155, 111, 90, 80, 35, 30, and 16°N) point at individual check dams located along the torrent (Figure 2d), indicating that, at Illgraben, coherent infrasound is radiated as the debris flows encounter check dams, which act as locations of preferential infrasonic radiation. Moreover, the long duration of the detection clusters (Figure 2) indicates that the infrasound radiation at check dams is not related just to flow front, whose passage through the dam is way shorter in time, but to the whole debris flow. Each check dam dominates the infrasonic radiation until the barycenter of the flow moves to a further downstream one, which at that time results as the new most powerful infrasonic source. Therefore, array processing allows to locate moment

by moment, along the torrent, the source of the most energetic infrasonic signal component recorded by the array (Figure 2d). It's worth noting that, sometimes (e.g., minutes 35–40 and 55–70) infrasonic detections from different check dams are recorded at the same time, revealing the co-presence of infrasonic sources of comparable energy in different positions (Figures 2c and 2d).

Moreover, the highest infrasonic amplitudes are recorded at back-azimuths between 155°N and 80°N (Figures 2b and 2c), corresponding to the channel sector located at the minimum distance from the recording sensors (between CD16 and CD22, Figure 2d), in agreement with findings by Marchetti et al. (2019). In particular, the infrasonic amplitude peaks for a back-azimuth equal to 111°N, corresponding to CD20, which, in addition to being one of the dams located closest to ILG array, is also the tallest dam (∼8 m high, Figure 1e) after CD1.

Obtained results, observed also for several Illgraben debris flows (Figure S2 in Supporting Information S1), represent a clear on-field confirmation of the infrasonic source mechanism suggested by Belli et al. (2022) for debris flows, according to which infrasound is radiated by turbulence-induced waves and splashes at the flow surface, whose formation is enhanced at significant channel irregularities (topographic steps and steep bends) (Chaudhry, 2008; Feng et al., 2014; Henderson, 1996; Tokyay & Yildiz, 2007). Among them, drops at check dams result as predominant infrasonic sources for Illgraben debris flows.

The observed sequential infrasound source migration differs significantly from the most active source of seismic energy, related to the boulder-rich flow front (Farin et al., 2019; Walter et al., 2017), further confirming the different source processes for the infrasonic and seismic radiation by debris flows.

4.3. The Seismo-Acoustic Cross-Correlation

The cross-correlation analysis reveals high correlation between infrasound and seismic signal during the entire debris flow in the 2–10 Hz frequency band (Figure 3c), while almost no correlation is recorded between 10 and 20 Hz (Figure 3f). The high seismo-acoustic correlation between 2 and 10 Hz indicates that the two wavefields, different from what is expected based on accepted source models (Section 1) and on the recorded spectral signatures (Figures 1g and 1i, Figure S1 in Supporting Information S1), are related to each other. Maximum correlation coefficients, ranging between 0.1 and 0.45, are observed for lag values (hereinafter lag_{MAX}) which vary during the event, between ∼0 and ∼1.9 s (Figure 4a). These positive lags indicate that the recorded seismic signal component precedes the cross-correlated infrasound throughout the event. Similar results are obtained also for other Illgraben debris flows, although the cross-correlation is more intense for smaller flows and less evident or even absent for larger ones (Figure S3 in Supporting Information S1).

Following the theoretical model by Ichihara et al. (2012), we can use the lag_{MAX} values of the seismo-acoustic cross-correlation to infer insights on the source processes. In particular, a $lag_{MAX} = 0$, as observed shortly after the event onset (between minutes 22 and 26; Figure 4a) is expected in case of secondary infrasound produced at the sensor by the transmission in the air of the primary incident seismic waves (i.e., seismoacoustic coupling) (Kim et al., 2004). Indeed, this phase of the debris flow is marked by a rapid increase of the seismic amplitude, compared to a more stable infrasonic one. The $lag_{MAX} / = 0$ observed for most of the event (Figures 3c and 3d) is instead consistent with the correlation between primary infrasonic and seismic signal components generated at the source (i.e., in the debris flow), and results from the different propagation velocities of the two wavefields. For the 2–10 Hz surface seismic waves, dominating the debris-flow seismic signal (Lai et al., 2018; Tsai et al., 2012), in agreement with the Illgraben shallow velocity model by Zhang, Walter, McArdell, Wenner, et al. (2021), we can assume a group velocity (v_{ss}) of 800–1,000 m/s. The infrasound instead propagates in the air at the speed of sound (c), which, at sea level, is ∼340 m/s (Kirtskhalia, 2012). As a consequence of the different propagation velocities, a common source position would result into seismic and infrasonic signals recorded with different times at the seismo-acoustic station. The delay time between the seismic signal and the infrasound (Δt_{s-i}), which determines the lag_{MAX} observed in the cross-correlation analysis, depends on the source-to-receiver distance (r) as:

$$\Delta t_{s-i} = r\left(\frac{1}{C} - \frac{1}{V_{ss}}\right) = lag_{MAX}. \quad (1)$$

Using Equation 1, and assuming v_{ss} = 900 m/s, the lag_{MAX} observed in the seismoacoustic cross-correlation function can be inverted to compute the source-to-receiver distance (Figure 4b), and thus to locate the seismo-acoustic source moment by moment along the torrent. The obtained localization is consistent with the

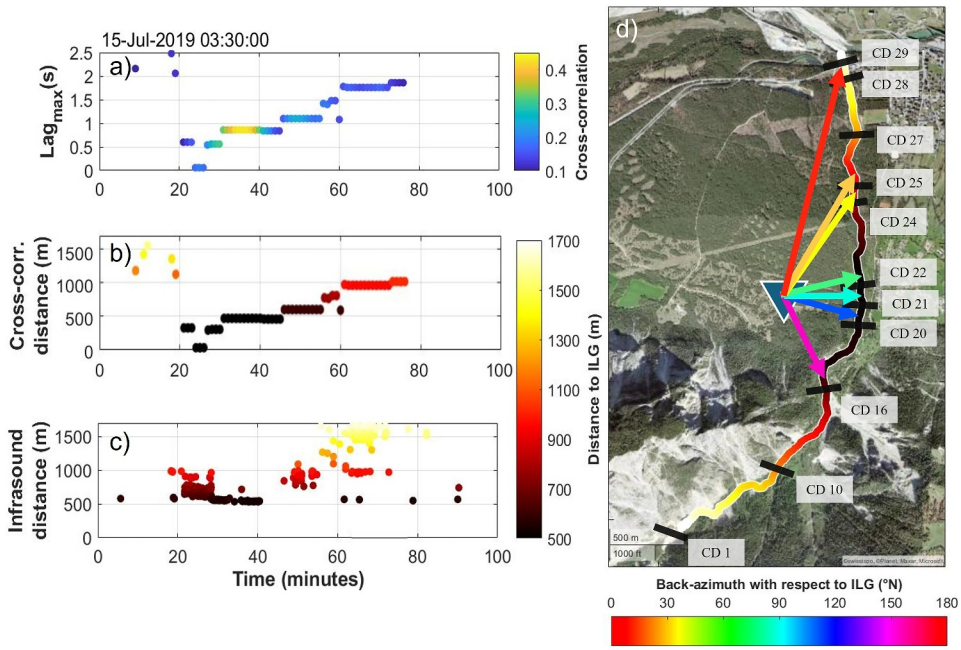

Figure 4. Time evolution of the lag_{MAX} derived from the seismo-acoustic cross-correlation (a): data points are colored according to their cross-correlation value. Time evolution of the source-to-receiver distance derived from the lag_{MAX} using Equation 1 (b). Time evolution of the source-to-receiver distance derived from the back-azimuth computed with the infrasonic array processing (c). Distances values in panels (b) and (c) are color-coded. Map of the Illgraben channel between CD1 and CD30 (d): Channel points are colored based on their distance from the seismo-acoustic sensors (blue triangle), according to the color bar beside diagrams (b) and (c). Arrows in panel (d) are color-coded by and point in the direction of the infrasonic back-azimuth (see Figure 2) according to the color bar below the map.

movement of the debris flow along the Illgraben channel (Figure 4d). Moreover, similar to what is observed for the recorded infrasonic back-azimuth (Figure 2c), the computed source-to-receiver distance shows a stepped variation over time (Figure 4), highlighting once again sources located in fixed positions along the channel for the correlated seismo-acoustic signal components.

Since each point of the Illgraben channel is characterized by specific values of backazimuth and distance with respect to the seismo-acoustic sensors (Figures 2d and 4d), the infrasonic back-azimuth obtained from array processing can be inverted to derive the evolution over time of the distance between the main source of the infrasonic signal and the recording array (Figure 4c). This inversion allows us to compare the localization of the source obtained only with infrasound, with the one obtained with the seismo-acoustic cross-correlation (Figure 4d). The comparison reveals a good agreement between the two methods and suggests that a common source mechanism for infrasound and seismic waves develops in the debris flow (high cross-correlation) at check dams (Figures 2d and 4e), which radiates energy that propagates with different velocity from the source to the receiver ($lag_{MAX} / = 0$) and migrates as the flow moves downhill (varying lag). This corroborates the findings by Wenner et al. (2019), who observed that the seismic spectral emission of Illgraben debris flows is affected by large topographic features, like check dams.

To explain the observed correlation, we suggest that an additional component of the recorded seismic signal, below 10 Hz, is produced by the turbulence structures developing downstream check dams (Ervine et al., 1997; Feng et al., 2014; Tokyay & Yildiz, 2007), which, according to previous studies (Belli et al., 2022; Marchetti et al., 2019) and to our array processing (Figure 2), are responsible also for the radiation of infrasound by debris flows. This agrees with Ervine et al. (1997), who observed that water jets impinging plunge pools at the base of dams generate turbulence-induced eddies, with dimensions up to the flow depth, which cause pressure oscillations at the floor. Turbulence structures have already been observed and modeled as seismic sources for rivers (Burtin et al., 2008; Gimbert et al., 2014; Schmandt et al., 2013). Therefore, such a source mechanism is expected to be active also within debris flows, despite being likely hidden by the dominant and more energetic seismic source related to the particle collisions with the riverbed (Farin et al., 2019; Lai et al., 2018).

More specifically, for the Illgraben, we suggest that the heavy flow turbulence triggered by water drop at check dams enhances there the formation of oscillations and waves at the flow surface. Such waves push the air, radiating infrasound, and, at the same time, determine variations of the stress exerted at the riverbed (Ervine et al., 1997; Gimbert et al., 2014), generating seismic waves. Both wavefields present a spectral content (<10 Hz) which reflects the periods of the eddies and of the oscillations at the flow surface, so that the generated infrasound and seismic waves are in phase and result correlated with each other. This turbulence-related seismic component adds to the more powerful one generated by the collisions between the transported solid particles and the riverbed, which represents the dominant seismic source mechanism in debris flows over a broader frequency band (Farin et al., 2019; Kean et al., 2015; Lai et al., 2018; Zhang, Walter, McArdell, Wenner, et al., 2021).

5. Conclusions

This work allows us to define additional constraints on the seismic and infrasonic radiation processes within debris flows. The array processing confirmed a preferential infrasonic radiation at check dams, not only associated to the passage of the flow front, but during the whole event (Figure 2). This agrees with the source mechanism proposed by Belli et al. (2022), attributing the radiation of infrasonic waves by debris flows to turbulence-induced waves and water splashes developing at the free surface of the flow downstream channel irregularities (Bedard, 2021; Chaudhry, 2008; Feng et al., 2014; Henderson, 1996).

Although the different frequency contents reveal different dominant source processes for the infrasonic and seismic signals generated by debris flows, the intense cross-correlation between primary seismo-acoustic signals observed during the event (Figure 3) outlines an unexpected relation between the two wavefields. More specifically, results suggest that, in addition to the main source of seismic energy due to particle collisions and mostly related to the flow front (Farin et al., 2019; Lai et al., 2018; Walter et al., 2017; Zhang, Walter, McArdell, Wenner, et al., 2021), a still significant component of the seismic signal produced by debris flows is likely generated by the powerful turbulence structures developing due to water drop at check dams (Ervine et al., 1997; Tokyay & Yildiz, 2007), which also produce infrasound (Belli et al., 2022; Feng et al., 2014). At Illgraben this is observed for the seismic component below 10 Hz. Our interpretation is consistent with the spectra computed on the seismic signals of the event recorded at ILL11 and ILL12 seismic stations deployed closer to the torrent at Illgraben, showing a slight enrichment between 2 and 10 Hz, following the trend observed for the infrasonic spectrum (see Section S4 in Supporting Information S1). We suggest that the turbulence-related seismic source in debris flows might be enhanced at Illgraben, because of the larger size of its check dams compared to other sites, which therefore trigger more energetic turbulence (Belli et al., 2022; Tokyay & Yildiz, 2007), and for smaller, less granular and more fluid events, because of the milder dominance of the collision-related source. This seems confirmed by the trend observed for other Illgraben debris flows, with the larger flows being characterized by lower seismo-acoustic cross-correlation (Figure S3 Supporting Information S1). The additional seismic source mechanism highlighted here opens new scenarios for future experimental and/or theoretical studies aimed at estimating the seismic component produced by flow-turbulence starting from the recorded infrasound, so as to be able to discriminate within the seismic signal the contributions associated to the different source processes (particle collisions and flow turbulence).

Eventually, our study further highlights the potential of using infrasonic and seismic signals for monitoring debris flows, as already indicated in previous studies (Marchetti et al., 2019; Belli et al., 2022; Schimmel & Hübl, 2016; Chmiel et al., 2021; Schimmel et al., 2022). If an infrasound antenna is available, the array processing has proven to be able to identify the debris flow passage at the main check dams located along the Illgraben channel (Figure 2), so that it can be used to detect and track events in real time, as already suggested by Marchetti et al. (2019). Similarly, our work shows how, if co-located infrasonic and seismic sensors are present, the seismo-acoustic cross-correlation analysis could be used to localize debris flows in well-known channels (Figure 4).

Data Availability Statement

Infrasound data are freely available at Belli (2024). Seismic data are openly available at Belli and Walter (2024).

References

Allstadt, K. E., Farin, M., Lockhart, A. B., McBride, S. K., Kean, J. W., Iverson, R. M., & George, D. (2019). *Overcoming barriers to progress in seismic monitoring and characterization of debris flows and lahars* (Vol. 28). Association of Environmental and Engineering Geologists; special publication. https://doi.org/10.25676/11124/173234

Acknowledgments
We are grateful to Doc. Brian McArdell for providing us with the flow parameters of the analyzed event. This study was carried out within the multidisciplinary project of the University of Florence "A new interdisciplinary approach to advance understanding of sediment and large wood TRANSport in FORESTED MOUNTAIN catchments – TRANSFORM", CUP B55F21007810001, funded within the PNR 2021-2027, funded by the European Union – Next Generation EU. The University of Florence acknowledges the contribution of the National Recovery and Resilience Plan, Mission 4 Component 2 Investment 1.4 NATIONAL CENTER FOR HPC, BIG DATA AND QUANTUM COMPUTING funded by the European Union NextGenerationEU CUPB83C22002830001. Open access publishing facilitated by Universita degli Studi di Firenze, as part of the Wiley - CRUI-CARE agreement.

Arattano, M., & Marchi, L. (2008). Systems and sensors for debris-flow monitoring and warning. *Sensors*, *8*(4), 2436–2452. https://doi.org/10.3390/s8042436

Badoux, A., Graf, C., Rhyner, J., Kuntner, R., & McArdell, B. W. (2009). A debrisflow alarm system for the alpine Illgraben catchment: Design and performance. *Natural Hazards*, *49*(3), 517–539. https://doi.org/10.1007/s11069-008-9303-x

Bedard, A. J. (2021). Waterfall low-frequency vibrations and infrasound: Implications for avian migration and hazard detection. *Journal of Comparative Physiology*, *207*(6), 685–700. https://doi.org/10.1007/s00359-021-01510-5

Belli, G. (2024). Ilg infrasound data [Dataset]. *OSF*. Retrieved from osf.io/9cmbt

Belli, G., Gheri, D., Bovet, E., Durand, N., Dellavedova, P., & Marchetti, E. (2025). Decennial infrasonic array analysis of snow-avalanche activity in Aosta Valley: New perspectives for supporting avalanche forecasting. *Cold Regions Science and Technology*, 104521. https://doi.org/10.1016/j.coldregions.2025.104521

Belli, G., Pace, E., & Marchetti, E. (2021). Detection and source parametrization of small-energy fireball events in western alps with ground-based infrasonic arrays. *Geophysical Journal International*, *225*(3), 1518–1529. https://doi.org/10.1093/gji/ggab042

Belli, G., & Walter, F. (2024). Ill13 seismic data [Dataset]. *OSF*, Retrieved from osf.io/vcfz9/andwww.orfeus-eu.org/data/eida/

Belli, G., Walter, F., McArdell, B., Gheri, D., & Marchetti, E. (2022). Infrasonic and seismic analysis of debris-flow events at Illgraben (Switzerland): Relating signal features to flow parameters and to the seismo-acoustic source mechanism. *Journal of Geophysical Research: Earth Surface*, *127*(6), e2021JF006576. https://doi.org/10.1029/2021JF006576

Berti, M., & Simoni, A. (2005). Experimental evidences and numerical modelling of debris flow initiated by channel runoff. *Landslides*, *2*(3), 171–182. https://doi.org/10.1007/s10346-005-0062-4

Bessason, B., Eir´ıksson, G., Thorarinsson, O´., Th´orarinsson, A., & Einarsson, S. (2007). Automatic detection of avalanches and debris flows by seismic methods. *Journal of Glaciology*, *53*(182), 461–472. https://doi.org/10.3189/002214307783258468

Burtin, A., Bollinger, L., Cattin, R., Vergne, J., & N´abˇelek, J. (2009). Spatiotemporal sequence of Himalayan debris flow from analysis of high-frequency seismic noise. *Journal of Geophysical Research*, *114*(F4), F04009. https://doi.org/10.1029/2008JF001198

Burtin, A., Bollinger, L., Vergne, J., Cattin, R., & N´abˇelek, J. (2008). Spectral analysis of seismic noise induced by rivers: A new tool to monitor spatiotemporal changes in stream hydrodynamics. *Journal of Geophysical Research*, *113*(B5), B05301. https://doi.org/10.1029/2007JB005034

Burtin, A., Hovius, N., McArdell, B., Turowski, J., & Vergne, J. (2014). Seismic constraints on dynamic links between geomorphic processes and routing of sediment in a steep mountain catchment. *Earth Surface Dynamics*, *2*(1), 21–33. https://doi.org/10.5194/esurf-2-21-2014

Chaudhry, M. H. (2008). *Open-channel flow* (Vol. 523). Springer.

Chmiel, M., Walter, F., Wenner, M., Zhang, Z., McArdell, B. W., & Hibert, C. (2021). Machine learning improves debris flow warning. *Geophysical Research Letters*, *48*(3), e2020GL090874. https://doi.org/10.1029/2020GL090874

Coco, M., Marchetti, E., & Morandi, O. (2021). Numerical modeling of infrasound energy radiation by debris flow events. *Pure and Applied Geophysics*, *178*(6), 2301–2313. https://doi.org/10.1007/s00024-021-02759-2

Coussot, P., & Meunier, M. (1996). Recognition, classification and mechanical description of debris flows. *Earth-Science Reviews*, *40*(3–4), 209–227. https://doi.org/10.1016/0012-8252(95)00065-8

Coviello, V., Arattano, M., Comiti, F., Macconi, P., & Marchi, L. (2019). Seismic characterization of debris flows: Insights into energy radiation and implications for warning. *Journal of Geophysical Research: Earth Surface*, *124*(6), 1440–1463. https://doi.org/10.1029/2018JF004683

de Groot-Hedlin, C., & Hedlin, M. (2019). Detection of infrasound signals and sources using a dense seismic network. *Infrasound Monitoring for Atmospheric Studies: Challenges in Middle Atmosphere Dynamics and Societal Benefits*, 669–700. https://doi.org/10.1007/978-3-319-75140-5_21

Delle Donne, D., Ripepe, M., De Angelis, S., Cole, P., Lacanna, G., Poggi, P., & Stewart, R. (2014). Chapter 9 thermal, acoustic and seismic signals from pyroclastic density currents and vulcanian explosions at Soufriere hills volcano, Montserrat. *Geological Society, London, Memoirs*, *39*(1), 169–178. https://doi.org/10.1144/M39.9

Dowling, C. A., & Santi, P. M. (2014). Debris flows and their toll on human life: A global analysis of debris-flow fatalities from 1950 to 2011. *Natural Hazards*, *71*(1), 203–227. https://doi.org/10.1007/s11069-013-0907-4

Ervine, D., Falvey, H., & Withers, W. (1997). Pressure fluctuations on plunge pool floors. *Journal of Hydraulic Research*, *35*(2), 257–279. https://doi.org/10.1080/00221689709498430

Farin, M., Tsai, V. C., Lamb, M. P., & Allstadt, K. E. (2019). A physical model of the high-frequency seismic signal generated by debris flows. *Earth Surface Processes and Landforms*, *44*(13), 2529–2543. https://doi.org/10.1002/esp.4677

Feng, H., Yang, Y., Chunchuzov, I., & Teng, P. (2014). Study on infrasound from a water dam. *Acta Acustica united with Acustica*, *100*(2), 226–234. https://doi.org/10.3813/AAA.918702

Gimbert, F., Tsai, V. C., & Lamb, M. P. (2014). A physical model for seismic noise generation by turbulent flow in rivers. *Journal of Geophysical Research: Earth Surface*, *119*(10), 2209–2238. https://doi.org/10.1002/2014JF003201

Havens, S., Marshall, H.-P., Johnson, J. B., & Nicholson, B. (2014). Calculating the velocity of a fast-moving snow avalanche using an infrasound array. *Geophysical Research Letters*, *41*(17), 6191–6198. https://doi.org/10.1002/2014GL061254

Henderson, F. M. (1996). *Open channel flow*. Macmillan.

Hicks, S. P., Matos, S. B., Pimentel, A., Belli, G., Gheri, D., Tsekhmistrenko, M., et al. (2023). Exclusive seismoacoustic detection and characterization of an unseen and unheard fireball over the North Atlantic. *Geophysical Research Letters*, *50*(22), e2023GL105773. https://doi.org/10.1029/2023gl105773

Ichihara, M., Takeo, M., Yokoo, A., Oikawa, J., & Ohminato, T. (2012). Monitoring volcanic activity using correlation patterns between infrasound and ground motion. *Geophysical Research Letters*, *39*(4), L04304. https://doi.org/10.1029/2011GL050542

Iverson, R. M. (1997). The physics of debris flows. *Reviews of Geophysics*, *35*(3), 245–296. https://doi.org/10.1029/97RG00426

Johnson, J., Anderson, J., Marshall, H., Havens, S., & Watson, L. (2021). Snow avalanche detection and source constraints made using a networked array of infrasound sensors. *Journal of Geophysical Research: Earth Surface*, *126*(3), e2020JF005741. https://doi.org/10.1029/2020JF005741

Kean, J. W., Coe, J. A., Coviello, V., Smith, J. B., McCoy, S. W., & Arattano, M. M. (2015). Estimating rates of debris flow entrainment from ground vibrations. *Geophysical Research Letters*, *42*(15), 6365–6372. https://doi.org/10.1002/2015GL064811

Kim, T. S., Hayward, C., & Stump, B. (2004). Local infrasound signals from the Tokachi-Oki earthquake. *Geophysical Research Letters*, *31*(20), L20605. https://doi.org/10.1029/2004gl021178

Kirtskhalia, V. G. (2012). Speed of sound in atmosphere of the earth. *Open Journal of Acoustics*, *2*(2), 80–85. https://doi.org/10.4236/oja.2012.22009

Kogelnig, A., Hübl, J., Surin˜ach, E., Vilajosana, I., & McArdell, B. W. (2014). Infrasound produced by debris flow: Propagation and frequency content evolution. *Natural Hazards*, *70*(3), 1713–1733. https://doi.org/10.1007/s11069-011-9741-8

Kogelnig, A., Surin˜ach, E., Vilajosana, I., Hübl, J., Sovilla, B., Hiller, M., & Dufour, F. (2011). On the complementariness of infrasound and seismic sensors for monitoring snow avalanches. *Natural Hazards and Earth System Sciences*, *11*(8), 2355–2370. https://doi.org/10.5194/nhess-11-2355-2011

Lai, V. H., Tsai, V. C., Lamb, M. P., Ulizio, T. P., & Beer, A. R. (2018). The seismic signature of debris flows: Flow mechanics and early warning at Montecito, California. *Geophysical Research Letters*, *45*(11), 5528–5535. https://doi.org/10.1029/2018GL077683

Le Pichon, A., Pilger, C., Ceranna, L., Marchetti, E., Lacanna, G., Souty, V., et al. (2021). Using dense seismo-acoustic network to provide timely warning of the 2019 paroxysmal stromboli eruptions. *Scientific Reports*, *11*(1), 1–12. https://doi.org/10.1038/s41598-021-93942-x

Liu, D., Leng, X., Wei, F., Zhang, S., & Hong, Y. (2018). Visualized localization and tracking of debris flow movement based on infrasound monitoring. *Landslides*, *15*(5), 879–893. https://doi.org/10.1007/s10346-017-0898-4

Liu, D., Leng, X.-P., Wei, F.-Q., Zhang, S.-J., & Hong, Y. (2015). Monitoring and recognition of debris flow infrasonic signals. *Journal of Mountain Science*, *12*(4), 797–815. https://doi.org/10.1007/s11629-015-3471-4

Marchetti, E., Lacanna, G., Le Pichon, A., Piccinini, D., & Ripepe, M. (2016). Evidence of large infrasonic radiation induced by earthquake interaction with alluvial sediments. *Seismological Research Letters*, *87*(3), 678–684. https://doi.org/10.1785/0220150223

Marchetti, E., Walter, F., Barfucci, G., Genco, R., Wenner, M., Ripepe, M., & Price, C. (2019). Infrasound array analysis of debris flow activity and implication for early warning. *Journal of Geophysical Research: Earth Surface*, *124*(2), 567–587. https://doi.org/10.1029/2018JF004785

Matoza, R. S., & Fee, D. (2014). Infrasonic component of volcano-seismic eruption tremor. *Geophysical Research Letters*, *41*(6), 1964–1970. https://doi.org/10.1002/2014gl059301

McArdell, B. W., Bartelt, P., & Kowalski, J. (2007). Field observations of basal forces and fluid pore pressure in a debris flow. *Geophysical Research Letters*, *34*(7), L07406. https://doi.org/10.1029/2006GL029183

Mutschlecner, J. P., & Whitaker, R. W. (2005). Infrasound from earthquakes. *Journal of Geophysical Research*, *110*(D1), D01108. https://doi.org/10.1029/2004JD005067

Novoselov, A., Fuchs, F., & Bokelmann, G. (2020). Acoustic-to-seismic ground coupling: Coupling efficiency and inferring near-surface properties. *Geophysical Journal International*, *223*(1), 144–160. https://doi.org/10.1093/gji/ggaa304

Schimmel, A., Coviello, V., & Comiti, F. (2022). Debris flow velocity and volume estimations based on seismic data. *Natural Hazards and Earth System Sciences*, *22*(6), 1955–1968. https://doi.org/10.5194/nhess-22-1955-2022

Schimmel, A., & Hübl, J. (2015). Approach for an early warning system for debris flow based on acoustic signals. In *Engineering geology for society and territory-volume 3: River basins, reservoir sedimentation and water resources* (pp. 55–58). https://doi.org/10.1007/978-3-319-09054-2_11

Schimmel, A., & Hübl, J. (2016). Automatic detection of debris flows and debris floods based on a combination of infrasound and seismic signals. *Landslides*, *13*(5), 1181–1196. https://doi.org/10.1007/s10346-015-0640-z

Schlunegger, F., Badoux, A., McArdell, B. W., Gwerder, C., Schnydrig, D., RiekeZapp, D., & Molnar, P. (2009). Limits of sediment transfer in an alpine debris-flow catchment, Illgraben, Switzerland. *Quaternary Science Reviews*, *28*(11–12), 1097–1105. https://doi.org/10.1016/j.quascirev.2008.10.025

Schmandt, B., Aster, R. C., Scherler, D., Tsai, V. C., & Karlstrom, K. (2013). Multiple fluvial processes detected by riverside seismic and infrasound monitoring of a controlled flood in the Grand Canyon. *Geophysical Research Letters*, *40*(18), 4858–4863. https://doi.org/10.1002/grl.50953

Tokyay, N. D., & Yildiz, D. (2007). Characteristics of free overfall for supercritical flows. *Canadian Journal of Civil Engineering*, *34*(2), 162–169. https://doi.org/10.1139/l06-114

Tsai, V. C., Minchew, B., Lamb, M. P., & Ampuero, J.-P. (2012). A physical model for seismic noise generation from sediment transport in rivers. *Geophysical Research Letters*, *39*(2), L02404. https://doi.org/10.1029/2011GL050255

Walter, F., Burtin, A., McArdell, B. W., Hovius, N., Weder, B., & Turowski, J. M. (2017). Testing seismic amplitude source location for fast debris-flow detection at Illgraben, Switzerland. *Natural Hazards and Earth System Sciences*, *17*(6), 939–955. https://doi.org/10.5194/nhess-17-939-2017

Wenner, M., Walter, F., McArdell, B., & Farinotti, D. (2019). *Deciphering debrisflow seismograms at Illgraben, Switzerland* (Vol. 28). Association of Environmental and Engineering Geologists; special publication.

Zhang, Z., Walter, F., McArdell, B. W., de Haas, T., Wenner, M., Chmiel, M., & He, S. (2021). Analyzing bulk flow characteristics of debris flows using their high frequency seismic signature. *Journal of Geophysical Research: Solid Earth*, *126*(12), e2021JB022755. https://doi.org/10.1029/2021jb022755

Zhang, Z., Walter, F., McArdell, B. W., Wenner, M., Chmiel, M., de Haas, T., & He, S. (2021). Insights from the particle impact model into the highfrequency seismic signature of debris flows. *Geophysical Research Letters*, *48*(1), e2020GL088994. https://doi.org/10.1029/2020GL088994